Proc. of the European Safety and Reliability Conference (ESREL 2026)
Edited by José C. Matos, Paulo B. Lourenço, Michael Beer, Daniel Oliveira, Edoardo Patelli, Hélder S. Sousa, Rui A. Silva and Monica Santamaria

doi: 10.3850/ESREL2026061419_esrel26-p26330-cd

A novel Physics-Based Causal Health Indicator for Fuel Cell Remaining Useful Life Online Estimation Under Dynamic Conditions

Misael Roatta
Univ. Grenoble Alpes, CEA, LETI, F-38000 Grenoble, France. E-mail: misael.roatta@cea.fr

Raphaël Morvillier
Univ. Grenoble Alpes, CEA, LETI, F-38000 Grenoble, France. E-mail: raphael.morvillier@cea.fr

Vincent Heiries
Univ. Grenoble Alpes, CEA, LETI, F-38000 Grenoble, France. E-mail: vincent.heiries@cea.fr

To increase the lifetime of fuel cell systems, a first step is to estimate their degradation and remaining useful life (RUL) by forecasting a health indicator (HI) until it reaches a threshold defining the end of life (EoL). In static applications, voltage or power are commonly selected as the HI. In dynamic applications, the relative power loss rate (RPLR) is considered more suitable. However, the RPLR is constructed from a simplified polarization model that does not take into account ohmic losses and is still too influenced by the short-term dynamics of the load profile. Other existing HIs based on more accurate models (stemming from physical laws to construct a Tafel-Ohmic model) cannot be computed online and do not take into account the current inside the fuel cell. To overcome the limitations of the available HIs, this work introduces a new physics-based HI based on inverting the Tafel-Ohmic model using the Lambert W function. This HI is compared to the existing ones using a pre-training metric measuring the global trend compared to local variation and a post-training metric measuring the RUL estimation performances. Compared to respectively the voltage and RPLR, the new HI has a 14 times and five times higher score in terms of global decreasing trend versus local, undesired, variations. Concerning the post-training results, it shows very good stability regarding the forecasting model parameters and has a RUL score 1.5 and 12 times higher than the voltage and RPLR, respectively.

Keywords: Health indicator, prognosis, remaining useful life, fuel cell, machine learning, Lambert function, Tafel equation, dynamic load, PEMFC

1. Introduction

Increasing the lifetime and reliability of proton exchange membrane fuel cells (PEMFCs) remains a major challenge to allow the massive deployment of PEMFCs that could in turn reduce the carbon footprint of transportation. Extending the fuel cell lifetime can be achieved with thanks to the following three-steps process: estimating its state of health (SoH), estimating its remaining useful life (RUL) and optimizing the fuel cell use and maintenance under environmental constraints with a control algorithm. This paper focuses on the first step of the process (SoH estimation), while the method for the second step has been described in Roatta et al. (2026) and will be used to validate the SoH estimation. To be used by the control algorithm, the SoH and RUL estimations must be performed online so the signal processing techniques applied must be causal, i.e., they are applied to past acquired data only.

1.1. *Definitions*

The SoH of a fuel cell quantifies the degradation level of the fuel cell relative to its initial performance at beginning of life (BoL). Mathematically, it is a monotonic variable decreasing from one, corresponding to the BoL, to a threshold defining the end of life (EoL). EoL is the moment at which the cell can no longer meet the required performance of its intended application due to irreversible degradation of its components. The SoH is not directly measurable in an online PEMFC, so a health indicator (HI) must be defined. A HI is a measurable variable (or combination of variables) that quantitatively reflects the current degradation state of the PEMFC and correlates with its SoH. Ideally, it should also be monotonically decreasing, but in practice, this is not the case due to recoveries (increases of the HI) and noise. A valid HI should be sensitive to degradation (changes consistently as the PEMFC ages), globally monotonic (consistently decreasing), correlated with the true SoH, noise-robust, easy to measure or estimate, causal (because the data will arrive in real-time). Also, the HI is ideally physically interpretable and linked to a known degradation mechanism.

1.2. *Experimental data*

The methods presented in this work are tested on data acquired during a durability test of around 2,300 operating hours using a 3-kW open-design metal stack (Häußler et al. (2024)). The experimental setup consists of a 10-cell short stack equipped with a current density measurement device. To replicate realistic operating conditions of heavy-duty applications, a mission profile consisting of a repeated 11.5-hours dynamic cycle is applied to the stack (Sanchez-Monreal et al. (2026)). To assess aging-related effects, polarization curves are recorded every 25 cycles. For heavy-duty transport applications, the target stack lifetime ranges from 20,000 to 30,000 operating hours. Previous tests indicate that degradation is initially high and non-linear during the first few hundred hours, then shifts to a slower and more linear regime after approximately 1,000–2,000 hours. This transition is observed within the test duration of this study. No further major change in degradation behavior is expected beyond the 2,300 measured operating hours; therefore, this dataset is considered representative.

1.3. *Static and dynamic conditions*

In static conditions (i.e., the current is almost constant), stack voltage or power satisfy the properties of a HI (Hua et al. (2022)). However, in dynamic conditions, voltage can no longer be the HI. In fact, the resulting measured voltage signal is a combination of four main phenomena: the instantaneous current command response provokes the **local variations** corresponding to the signal high frequencies; the long-term response associated with irreversible degradation mechanisms leads to a **global decreasing trend** corresponding to the signal's low frequencies; **sudden recoveries** provoked by reversible degradation during characterization measurements (e.g., polarization curve) create some significant and local increases of the voltage; and finally, different **noises** due to measurement limitations or exceptional abnormal behaviors disturb the signal. For the RUL estimation task, the global decreasing trend and the sudden recoveries are of primary interest, while the local variations and noises are out of interest and can even bias an estimation. The major challenge in dynamic conditions is that the global decreasing trend is negligible compared to the local variations. In the literature (Hua et al. (2022)), the electrochemical surface area (ECSA) can be used as a good HI because it is well correlated to the SoH. However, ECSA measurement is challenging to perform in embedded applications (e.g., in vehicles), limiting its applicability for this use case.

2. Health Indicators Extraction Methods

In this study, three HI extraction methods relying on equations are investigated. The used equations all include a notion of degradation and use current and voltage as input. In Section 3, two equations will be examined. The three methods presented here are different ways of obtaining a HI by calibrating the equations with real data. The difference between the three methods is mainly the temporal frequency of the calibration. The first one, in Section 2.1, is not computable online and is used as an accurate benchmark comparison.

2.1. *Polarization curve method*

Usually, during the durability tests, polarization curves measurements are performed regularly. The *polarization curve* method (*PC*) consists of fitting each of the polarization curves to the equation and then fitting a decreasing time-depending logarithm model described in Eq. (1) (t corresponds to the time and A, B, C, and D are the parameters to fit).

$$HI_{\mathrm{PC}}(t) = 1 - A\ln(Bt + C) - D \qquad (1)$$

This method does not use the real-time aging data, and polarization curves cannot be measured online at any time because it is a long and intrusive process. Consequently, it does not take into account the sudden recoveries, but it provides an accurate degradation estimation each time a polarization curve measurement is done, for comparison.

2.2. *Cycle method*

The *cycle* method can be applied when the current load is a repeated short-term dynamic cycle. It considers that each cycle in the aging data is equivalent to a polarization curve on which the equation is fitted. The hypothesis is that current values, in a single cycle, are sufficiently spread to be considered as a valid polarization curve. Then, the HI can be calculated at each cycle.

2.3. *Real-time method*

The *real-time* method (*RT*) consists of inverting the equation analytically. More precisely, this type of equation often gives the voltage (or power) as a function of the current and some additional parameters. First, the objective is to express these additional parameters as a function of the HI by introducing long-term degradation mechanisms or empirical models. Then, inverting the equation allows obtaining another equation giving the HI as a function of the voltage and current. This method allows obtaining a real-time value of the HI at the same sampling frequency as the voltage and the current. First, because the equation is not accurate for null current values, an outlier removal is performed thanks to a moving-median z-score detection. Then, to reduce computational training cost of the RUL estimation machine learning model describes in Section 4.3, a causal moving average filter followed by a sub-sampling is applied.

3. Models Equations

Modeling the PEMFC behavior can be achieved with more or less complex equations depending on which information we want to extract or the domain of validity. In dynamic conditions, equations modeling steady-state and transient behavior should be used (Saadi et al. (2017)). However, these equations are complex, too difficult to calibrate accurately, and even worse to invert analytically. Moreover, the higher precision they provide is not required by the RUL estimation final task, and under some checked hypotheses, extended-static equations are suitable. In the case of using static models, polarization curve equations are used. The polarization equation can be empirical, for example, a sinus model of power (Hua et al. (2021)). Alternatively, it can be derived by applying fundamental physical laws (Jouin et al. (2016)). Normally, in the case of static models, all the environmental conditions are considered constant (Tzelepis et al. (2021)). However, these models can also be used in dynamic conditions by adding a notion of degradation varying through time represented by the HI. To determine which parameter(s) of the equation can be assimilated to the HI, a sensitivity analysis on the parameters of the equation (described in Section 3.1) is performed in the case of the empirical sinus model of power, and physical knowledge is used for the case of the physical equation.

3.1. *Sinus empirical model of power*

The simplest model is the sinus empirical model of power defined in Hua et al. (2021) (see Eq. (2), where P is the power, I is the current, and a, b, and c are the parameters to calibrate).

$$P(I) = a\sin(bI + c) \qquad (2)$$

The objective is to define a HI from this equation. Since Eq. (2) can be calibrated at every moment of the PEMFC life with a polarization curve, the evolution of the parameters with time is studied. Multiple assumptions are made on which parameters vary with time (and hence with degradation). We can then check which assumption is the most aligned with the polarization curves. For that, for each polarization curve, the root mean squared reconstruction error is calculated, and then an average and standard deviation are computed over all the obtained values, for each assumption. The results are presented in Table 1. Concerning the

Table 1. Results of sensitive analysis (averaged reconstruction error) on the calibration of the sinus model on polarization curves through time.

Free parameters	$a\ b\ c$	$b\ c$	$a\ c$	$a\ b$	c	b	a
Averaged error (W $\cdot 10^{-1}$)	1.9	3.4	2.6	2.0	7.0	4.1	3.3
Standard deviation (W $\cdot 10^{-1}$)	0.15	0.80	0.45	0.17	2.4	1.1	0.78

assumptions, all the possible combinations of free parameters are tested. For example, if we consider that all the parameters can vary with degradation, we fit Eq. (2) with a, b, and c and we obtain very good alignment of the model with the polarization curves (column one of Table 1). If we constrain one parameter to be constant (i.e., two parameters are free, and this corresponds to columns two, three, and four of Table 1), the model is less accurate, but the best case (a and b free) shows comparable performance to the three free parameters case. Finally, if only one parameter is set free (corresponding to columns five, six, and seven of Table 1), the best case is obtained when a is set free. This means that, if there were to be only one parameter to change over time to reflect the degradation, the best choice would be a. Even if the reconstruction error and deviation are much higher than the two free parameters best case, this configuration is chosen because the analytical inversion of Eq. (2) with a and b as free parameters is too complex. As a is decreasing over time, it is directly expressed as $a = a_0 HI$ to satisfy the properties of a HI. Then, the way to compute the HI in real-time is obtained by combining this definition with Eq. (2) to obtain Eq. (3) with $a_0 \neq 0$ and $0 < bI + c \leq \frac{\pi}{2}\ \forall I$.

$$HI_{\text{sinus}}(U, I) = \frac{UI}{a_0 \sin(bI + c)} \tag{3}$$

Note that this choice corresponds to the state-of-the-art HI relative power loss rate (RPLR) defined in Hua et al. (2021).

3.2. *Tafel-Ohmic equation of voltage*

Another solution is to use a less empirical and more physical equation, called Tafel-Ohmic in this paper. It remains very simple and models not the power anymore but the voltage (see Jouin et al. (2016), Eq. (4) where U_0 is the reversible voltage, R is the gas constant, T is the operating temperature, F is the Faraday constant, a is the charge transfer coefficient of the electrodes, i_{loss} is the stack internal current, i_0 is the exchange current at the electrodes, R_{eq} is the equivalent ohmic resistance, B_c is an empirical parameter, and i_L is the limiting current at the cathode).

$$\begin{aligned} U(I) = U_0 - \frac{RT}{2aF} \ln\left(\frac{i_{\text{loss}} + I}{i_0}\right) \\ -IR_{eq} - B_c \ln\left(1 - \frac{I}{i_L}\right) \end{aligned} \tag{4}$$

The objective is then to find which parameter embeds the degradation phenomena. In light of the work performed in Yue et al. (2022) based on the physics of the degradations, three parameters can be considered as potential candidates to embed degradation: R_{eq}, i_0, and i_L. The fitting of the polarization curve at BoL results in a null value of B_c, meaning that the concentration term is negligible compared to the ohmic loss and the activation loss. This means i_L is not present in the equation anymore. Moreover, the calibration with the polarization curves shows that both remaining parameters are varying with time, R_{eq} is increasing, and i_0 is decreasing. Also, the sum of the two parameters is approximately constant and equal to two. We can express the two parameters as a function of a single variable satisfying the properties of a HI: $i_0 = i_{0,init} HI$ and $R_{eq} = R_{eq,init}(2 - HI)$. The final equation is visible in Eq. (5) with $A = \frac{RT}{2aF}$.

$$\begin{aligned} U(HI, I) = U_0 - A \ln\left(\frac{i_{\text{loss}} + I}{i_{0,\text{init}} HI}\right) \\ - IR_{eq,\text{init}}(2 - HI) \end{aligned} \tag{5}$$

To obtain the HI at any time, the equation needs to be inverted analytically, as introduced in Section 2.3. This inversion can be done thanks to the multivalued Lambert W function (see Corless et al. (1996)). W is defined as the inverse of the function $f(w) = we^w$. As f is not injective, the solution W has several branches. Starting from Eq. (5), we isolate the terms containing HI to obtain:

$$A\ln(HI) + IR_{eq,init}HI = C \tag{6}$$

with

$$C := 2IR_{eq,init} + U - U_0 + A\ln\left(\frac{i_{loss} + I}{i_{0,init}}\right)$$

a constant with respect to HI. Then, we divide Eq. (6) by $A \neq 0$ and apply the exponential function to obtain Eq. (7).

$$HI\exp\left(\frac{IR_{eq,init}}{A}HI\right) = \exp\left(\frac{C}{A}\right) \tag{7}$$

Finally, we multiply by $\frac{IR_{eq,init}}{A}$, define $w = \frac{IR_{eq,init}HI}{A}$, and obtain Eq. (8).

$$we^w = \frac{IR_{eq,init}}{A}\exp\left(\frac{C}{A}\right) := z \tag{8}$$

As z is positive, the function f is actually injective in those boundaries. Therefore, we can define the HI shown in Eq. (9) with the principal branch $w = W_0(z)$, with $i_{loss} \neq 0$ and $i_{0,init} \neq 0$.

$$HI_{\text{Tafel}}(U, I) = \begin{cases} \frac{A}{IR_{eq,\text{init}}}W_0(z(U, I)), & I \neq 0, \\ \frac{i_{\text{loss}}}{i_{0,\text{init}}}\exp\left(\frac{U_0 - U}{A}\right), & I = 0. \end{cases} \tag{9}$$

4. Results

Three HI extraction methods and two equations have been presented and are summarized in Table 2. The sampling period is taken equal to 15 minutes. Since the true EoL is not reached during the tests, an *artificial* EoL is defined at the end of the available data, and the corresponding HI threshold is used as the EoL threshold. A min–max normalization is applied to the HIs to improve visualization in the figures, but it is not used for the metric computation or for the algorithm training and validation.

4.1. *Graphical comparison*

Figure (1) shows a visual comparison of the *cycle* and *polarization curve* HIs. The *polarization curve* method leads to almost the same aging curve for both equations (see the full lines, both of them model the same global decreasing trend). Moreover, the *cycle* methods dots are following the trend of the *polarization curve* method curves. This validates the hypothesis of considering each cycle as an equivalent polarization curve. The advantage is that we can compute the HI more frequently and get some information about local degradation, such as the sudden recovery after each polarization curve measurement. Note that from about 100 cycles until the EoL, the Tafel-Ohmic orange dots are closer to the accurate *polarization curve* method curve compared to the *sinus* blue dots. Furthermore, Figure (2) compares the *real-time* and *cycle* methods with the preprocessed voltage (in grey). We can observe that the *real-time-sinus* HI (in blue) and the *real-time-Tafel* HI (in orange) both exhibit less local variations than the preprocessed voltage (in grey). Thus, the global decreasing trend of the HI stands out more compared to the local variations.

4.2. *Pre-training metric*

Contrary to the raw voltage, a good HI should have a global decreasing trend standing out more compared to the local variations. To measure this improvement, the *global vs local slope* score, pre-

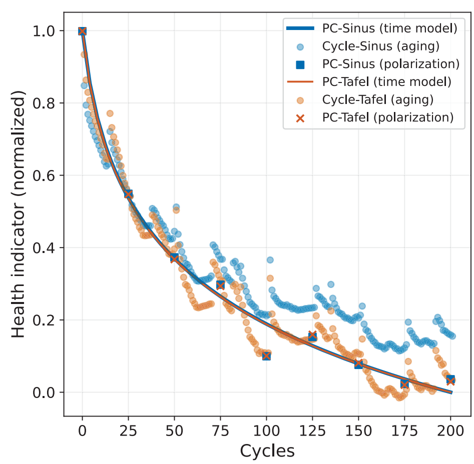

Fig. 1. Comparison of HI obtained with *cycle* and *polarization curve* methods. For a better visualization, a min-max normalization is performed to scale the HIs between 0 and 1.

Table 2. Assessment of the characteristics of the three HI computation methods studied in this work.

Method	Polarization curves	Cycles	Real-time
Initial sampling period	T = 25 cycles	T = 1 cycle $\approx$ 11.5 hours	T = 1 second
Data used	Polarization curve	Aging data on one cycle	One sample of aging data
Sinus model	fit of Eq. (2), (1)	fit of Eq. (2)	Evaluation of Eq. (3)
Tafel-Ohmic model	fit of Eq. (5), (1)	fit of Eq. (5)	Evaluation of Eq. (9)

sented in Eq. (10), is considered.

$$S = \frac{|\text{global slope}|}{\frac{1}{N}\sum_i |d_i|} \tag{10}$$

The global slope (numerator) is obtained thanks to a global linear regression on the whole data. Then, the local slope (denominator) is obtained by averaging all the absolute values of the local differences d_i between each data point. The score is computed on each HI as well as on the pre-processed voltage (same pre-processing as described in 2.3). Table 3 indicates the *gain* compared to the voltage *global vs local slope* score. The comparison can only be done across the equations (Sinus and Tafel-Ohmic) and not across the methods because they have different sampling frequencies. For the *polarization curve* and *cycle* methods, the gain is similar or almost similar between both equations. However, concerning the *real-time* method, the Tafel-Ohmic equation gain on the score is five times higher than the sinus one. Thereby, the *real-time-Tafel* HI is promising for the prognostic step.

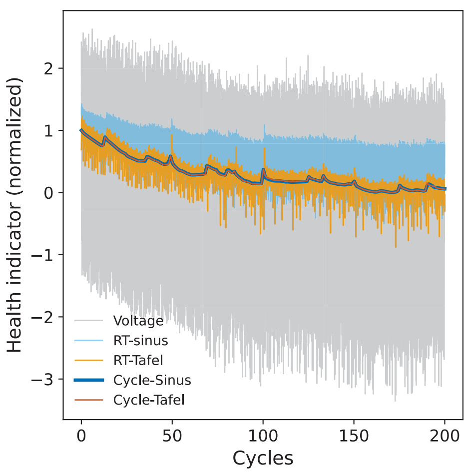

Fig. 2. Comparison of HI obtained with *cycle* and *real-time* methods. For a better visualization, a min-max normalization is performed to scale the HIs between 0 and 1.

Table 3. Gain on *Global vs local slope* score on the HIs compared to the voltage's score.

	Sinus	Tafel-Ohmic
Polarization curves	$8.0 \cdot 10^3$	$8.0 \cdot 10^3$
Cycles	$2.4 \cdot 10^3$	$2.3 \cdot 10^3$
Real-time	2.7	14

4.3. *Post-training metric*

Now that a satisfying HI has been defined, its effectiveness must be validated in the second step of the prognosis: estimating the RUL. This task cannot be achieved with the *polarization curve* method because the time-depending model is fitted *a posteriori* on all the polarization curves. The RUL estimation consists in performing a recursive forecasting of the HI thanks to a machine learning model trained on past data (and eventually historical data of other PEMFC when available), whose complete methodology is described in Roatta et al. (2026). The recursive forecasting is repeated until reaching the EoL threshold. The main input of the machine learning model is the HI computed in the past. In the case of the *real-time* method, the input also includes the current in the past and in the future until EoL. It is not relevant to include the current for the *cycle* method because there is no variation from one cycle to another. In the following example, we perform the forecasting starting from cycle 175 (approximately after 2,000 hours). We use all the available data before to train the machine learning model (train set) and the remaining data (approximatively 300 hours) to measure the RUL estimation performances (test set).

Roatta et al. (2026) shows that under data-scarce conditions, a simple linear model is sufficient to obtain a reliable estimation of the RUL; therefore, this model is adopted in this work. The lengths of the input and output windows of the recursive linear model must be chosen wisely because they determine the number of lags on which the output can depend. Fifty experiments are created by evenly choosing the input and output window lengths between 15 minutes and 25 hours each. The results of the 50 experiments are analyzed to study the robustness of the linear model training. It is impossible to compare metrics between forecasting two different HIs because the HIs' nature, order of magnitude, and noise are not comparable. Thereby, only the RUL estimation error described in Eq. (11) and the RUL curves are used to compare the performances of the different HIs forecasting.

$$\epsilon_k = \frac{|t_{k,\mathrm{EoL}} - \hat{t}_{k,\mathrm{EoL}}|}{t_{k,\mathrm{EoL}}} \tag{11}$$

$\hat{t}_{k,\mathrm{EoL}}$ is the estimation of the PEMFC EoL and $t_{k,\mathrm{EoL}}$ its real value. Several forecastings until EoL are performed, with starting points evenly distributed on the test set. To account for the cases when the RUL cannot be estimated because the forecasted HI never reaches the EoL threshold, we do not average the RUL estimation error directly but the reversed one. In this way, the term corresponding to the absence of RUL estimation is set equal to zero. The final metric is presented in Eq. (12), and has to be maximized.

$$\mathcal{S}_{\mathrm{RUL}} = \frac{1}{s}\sum_{k=1}^{s}\begin{cases}\frac{1}{\epsilon_k}, & \text{if } \hat{t}_{k,\mathrm{EoL}} \text{ detected,}\\ 0, & \text{otherwise.}\end{cases} \tag{12}$$

The number s corresponds to the number of forecasting that are performed until EoL. Figure (3) presents the results of the 50 experiments for each method. The *real-time-Tafel* method presents the highest and most stable scores at the same time, right before the pre-processed voltage, the *cycle-Tafel*, the *real-time-sinus*, and finally the *cycle-sinus* method. The final RUL curve of each best case is visible in Figure (4). This plot reveals that the *real-time-Tafel* method (orange, rounds) and both *cycle* methods (squares) show similar performances closer to the EoL. The *real-time-Tafel* method performs better when the prediction is further from EoL.

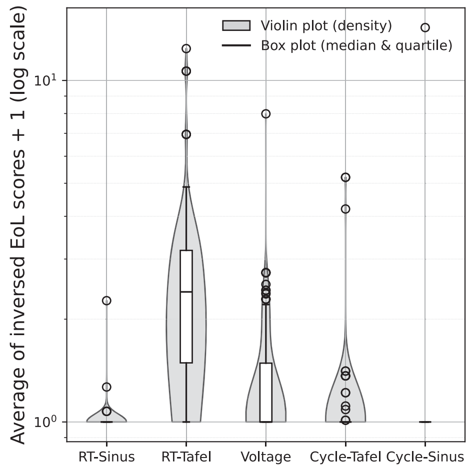

Fig. 3. Results of the 50 RUL estimation tests with different values of input and output windows lengths for the *cycle* and *real-time* methods, compared to the preprocessed voltage. Higher values are better.

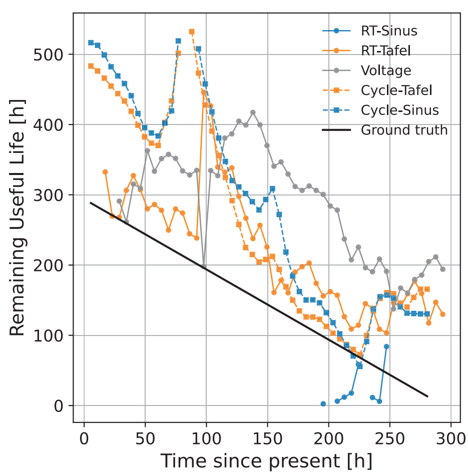

Fig. 4. RUL curve of the best RUL score obtained for each HI of the *cycle* and *real-time* methods compared to the preprocessed voltage, on the last 300 hours. The gaps correspond to prediction where no EoL has been detected i.e. the predicted HI never crosses the threshold.

5. Conclusion and Perspectives

This work presents a new HI calculation method, named *real-time-Tafel*, based on the Tafel-Ohmic static equation model in which we include degradation. The equation is inverted thanks to the Lambert W function and then processed to remove local variations and noise. The obtained HI is compared to other state-of-the-art HIs: the *cycle-Tafel* HI proposed in Yue et al. (2022) and the *real-time-sinus* HI also known as RPLR in Hua et al. (2021). For the *real-time* method, the Tafel-Ohmic HI outperforms the voltage and sinus HIs, with a fourteen and five times higher gain of global decreasing trend, respectively. Also, post-training results of this HI are promising because they show a RUL score 1.5 and 12 times higher than the voltage and sinus HIs, respectively. The RUL score is also more stable with respect to the input and output windows lengths. This HI is computable online with real-time data and takes into account the current, making it better suited to dynamic applications. This work advocates that defining relevant HIs is currently more critical than focusing on developing increasingly more complex models to forecast unsuitable HIs. As this work has only been applied to a unique dataset, further tests on multiple and diverse datasets is needed to validate the approach. This highlights the fact that data scarcity remains a critical issue in the field.

Acknowledgement

This work was performed within the framework of the RealHyFC (2023) project supported by the Clean Hydrogen Partnership and its members Hydrogen Europe and Hydrogen Europe Research under GA 101111904. The authors would like to thank especially Eva Fensterle PhD student at ZSW who has provided the durability dataset used in this study, and also partners of the consortium from CEA-LITEN, DLR, ZSW, and University of Ljubljana for discussions on data and models.

References

Corless, R. M., G. H. Gonnet, D. E. G. Hare, D. J. Jeffrey, and D. E. Knuth (1996). On the lambert W function. *Advances in Computational Mathematics 5*(1), 329–359.

Häußler, F., B. Wiedemann, C. Bergbreiter, S. Schneider, L. König, B. Cerne, E. Keller, F. Wilhelm, J. Scholta, and L. Jörissen (2024). The zsw hyfab generic stack: state-of-the-art and open pem fuel cell stack platform. Zenodo.

Hua, Z., Z. Zheng, E. Pahon, M.-C. Péra, and F. Gao (2021). Remaining useful life prediction of pemfc systems under dynamic operating conditions. *Energy Conversion and Management 231*, 113825.

Hua, Z., Z. Zheng, E. Pahon, M.-C. Péra, and F. Gao (2022). A review on lifetime prediction of proton exchange membrane fuel cells system. *Journal of Power Sources 529*, 231256.

Jouin, M., R. Gouriveau, D. Hissel, M.-C. Péra, and N. Zerhouni (2016). Degradations analysis and aging modeling for health assessment and prognostics of pemfc. *Reliability Engineering System Safety 148*, 78–95.

RealHyFC (2023). Realhyfc. Consulted on january the 5th, 2026.

Roatta, M., R. Morvillier, and V. Heiries (2026). Remaining useful life estimation of fuel cells using machine learning – a methodology. Working Paper in press, EHEC proceedings.

Saadi, A., M. Becherif, D. Hissel, and H. Ramadan (2017). Dynamic modeling and experimental analysis of pemfcs: A comparative study. *International Journal of Hydrogen Energy 42*(2), 1544–1557.

Sanchez-Monreal, J., J. Mitzel, C. Vacquier, and P. Gazdzicki (2026). Application relevant load cycles for pemfc component development and hybrid system optimization. *Energy Conversion and Management 348*, 120604.

Tzelepis, S., K. A. Kavadias, G. E. Marnellos, and G. Xydis (2021). A review study on proton exchange membrane fuel cell electrochemical performance focusing on anode and cathode catalyst layer modelling at macroscopic level. *Renewable and Sustainable Energy Reviews 151*, 111543.

Yue, M., Z. Li, R. Roche, S. Jemei, and N. Zerhouni (2022). Degradation identification and prognostics of proton exchange membrane fuel cell under dynamic load. *Control Engineering Practice 118*, 104959.